Experimental demonstration of decoherence-induced spontaneous symmetry breaking

Yun-Feng Huang, Liang Peng, Li Li, Bi-Heng Liu, Chuan-Feng Li,* and Guang-Can Guo

Key Laboratory of Quantum Information, University of Science and Technology of China, CAS, Hefei 230026, People's Republic of China

(Received 11 February 2011; published 3 May 2011)

We experimentally investigate the variations of exchange-symmetry properties of the four Bell states in an exchange-symmetric pure dephasing process with a two-photon system generated from spontaneous parametric down-conversion (SPDC). Experiment results show that under such an exchange-symmetric local-noise Hamiltonian, the exchange-symmetry property remains unchanged for two of the three symmetric Bell states, i.e., the states $|\Phi\rangle^{\pm} = \frac{1}{\sqrt{2}}(|00\rangle \pm |11\rangle)$. For the antisymmetric Bell state $|\Psi\rangle^{-} = \frac{1}{\sqrt{2}}(|01\rangle - |10\rangle)$, the exchange-symmetry property increases and achieves a maximum value of 0.5 at the asymptotic limit. However, for the third exchange-symmetric Bell state $|\Psi\rangle^{+} = \frac{1}{\sqrt{2}}(|01\rangle + |10\rangle)$, the exchange-symmetry property breaks, surviving with a probability of 0.5 at the asymptotic limit, which provides some evidence supporting such decoherence-induced spontaneous-symmetry-breaking phenomena.

DOI: 10.1103/PhysRevA.83.052105 PACS number(s): 03.65.Yz, 42.50.Dv, 42.50.Xa

I. INTRODUCTION

Quantum entanglement [1], as one of the characteristic features of quantum mechanics, has been playing a key role in the field of quantum information research and is responsible for many important and interesting protocols in quantum information processing, such as quantum teleportation [2], quantum cryptography [3,4], superdense coding [5], and quantum computation [6–8]. Quantum-entangled states have also been recognized as valuable resources for quantum-information-processing tasks. Unfortunately, this mysterious feature of composite quantum systems is very fragile when these systems are inevitably disturbed by the external environment in the real world. This has become the main obstacle to progress in realizing large-scale quantum information processing, e.g., long-distance quantum communication [9] or efficient quantum computation [10].

The destruction of entanglement by the interaction between quantum systems and the environment is essentially a "decoherence" [11] process, through which the coherent superpositions of quantum states are destroyed. In the last decade, the problem of decoherence has been extensively studied in various aspects [12–15] due to its importance for quantum-information-processing tasks and also for possible new insights into the foundations of quantum mechanics [16]. In recent years, the problem of relations between decoherence and spontaneous symmetry breaking has drawn much attention [17–19]. And more recently, an interesting theoretical result about decoherence-induced spontaneous symmetry breaking on entangled states was presented by Karpat and Gedik [20]. They studied the time evolution of the exchange-symmetry property of Bell states under an exchange-symmetric decoherence model and found a rather unexpected result: Not all three of the exchange-symmetric Bell states preserve their symmetry. The symmetry of Bell state $|\Psi\rangle^{+} = \frac{1}{\sqrt{2}}(|01\rangle + |10\rangle)$ breaks even when the decoherence model is exchange-symmetric, i.e., the model has a Hamiltonian invariant upon swapping the 2 qubits.

In this paper, we present an experiment that provides some evidence for supporting such decoherence-induced spontaneous-symmetry-breaking effects. Due to its robustness against environmental noise and its good controllability, the photonic system has been a very good choice for experimental research on decoherence [21]. So we used two-photon Bell states in our experiment and investigated the evolution of their exchange symmetry after a symmetric decoherence process was imposed on them. The experiment results show that the two symmetric Bell states $|\Phi\rangle^{\pm} = \frac{1}{\sqrt{2}}(|00\rangle \pm |11\rangle)$ kept their symmetry unchanged, while the third symmetric Bell state $|\Psi\rangle^{+}$ lost its symmetry and had a maximum probability 0.5 of being found symmetric at the asymptotic limit, which is in good accordance with theoretical prediction [20]. In addition, we imposed the same decoherence environment on the antisymmetric Bell state $|\Psi\rangle^{-} = \frac{1}{\sqrt{2}}(|01\rangle - |10\rangle)$, and the experiment result shows that the probability of being found in a symmetric state increases to 0.5 at the asymptotic limit.

II. THEORETICAL CALCULATIONS

In our experiment, we chose two-photon Bell states generated from the spontaneous parametric down-conversion (SPDC) process to undergo the decoherence. As mentioned above, photons are usually robust against decoherence, so for the sake of introducing a controllable decoherence model, we can utilize the many degrees of freedom (DOFs) of photons: polarization, frequency, momentum, etc. Such a decoherence model of coupling between polarization and frequency was first discussed by Berglund in Ref. [22]. If we consider the qubit encoded on only certain DOFs, then the other DOFs can be treated as the "environment" [23]. Thus, through some special method, the coupling between different DOFs of photons would lead to decoherence of the encoded qubit.

One method that has been frequently applied in experiments studying the decoherence of photonic systems is the nondissipative coupling between polarization and frequency DOFs of photons in a birefringent medium [21,24]. Here we encode the qubits on the polarization DOF and adopt the

*cfli@ustc.edu.cn

photon's frequency spectrum as the environment. The coupling between them is introduced by passing the photons through birefringent quartz plates. The different group velocities of the two orthogonal polarization modes in the quartz crystal and the nonzero photon-frequency-spectrum bandwidth result in decoherence of the polarization qubits. And we can well control the decoherence process by changing the thickness of quartz plates (evolution time) and also the spectrum of photons (the environment's features), thus providing a controllable decoherence model.

The initial two-photon entangled states generated by the SPDC process can be written as

$$|\psi(0)\rangle = |\Psi\rangle_{AB} \otimes \int g(\omega_1,\omega_2)|\omega_1\rangle_A|\omega_2\rangle_B d\omega_1 d\omega_2,,$$

where $|\Psi\rangle_{AB}$ is the 2-qubit entangled state encoded in the polarization DOF, and the subscripts A and B denote photons in spatial modes A and B. In the following discussion we will focus on the four Bell states $|\Phi\rangle^{\pm}_{AB}$ and $|\Psi\rangle^{\pm}_{AB}$. The integral part of the previous equation describes the initial state in the frequency DOF, i.e., the decoherence "environment"; and $g(\omega_1,\omega_2)$ is the amplitude corresponding to state $|\omega_1\rangle_A|\omega_2\rangle_B$, satisfying the normalization condition

$$\int |g(\omega_1,\omega_2)|^2 d\omega_1 d\omega_2 = 1.$$

In the normal experiment condition of SPDC, $g(\omega_1,\omega_2)$ can be written as

$$g(\omega_1,\omega_2) = h_A(\omega_1)h_B(\omega_2)a_p(\omega_p)\varphi(\omega_p,\omega_1-\omega_2),$$

where $h_A(\omega_1)$ and $h_B(\omega_2)$ are frequency amplitude functions of photon A and photon B, usually decided by narrow band filters placed in the paths of photon A and B, $a_p(\omega_p)$ is the frequency amplitude function of the pump light in SPDC, and $\omega_p = \omega_1 + \omega_2$ is the energy conservation relation in the SPDC process. The last factor, $\varphi(\omega_p,\omega_1-\omega_2)$, is the phase-matching function related to the details of phase-matching type and length of the down-conversion crystal. Here we can assume that the down-conversion crystal is thin; thus the constraint imposed by $\varphi(\omega_p,\omega_1-\omega_2)$ is weak and can be neglected. So $g(\omega_1,\omega_2)$ can be rewritten as $g(\omega_1,\omega_2) = h_A(\omega_1)h_B(\omega_2) a_p(\omega_p)$.

The decoherence coupling between the polarization and frequency DOFs is introduced by passing photon A and photon B through two quartz plates of length L_1 and L_2, respectively. And the two quartz plates are both oriented in such a way that the optical-path length for horizontal (or vertical) polarization mode is $n_H L$ ($n_V L$) after passing through an L-length quartz plate.

Now let us consider the case when the initial polarization state is $|\Psi\rangle^{+}_{AB} = \frac{1}{\sqrt{2}}(|HV\rangle + |VH\rangle)_{AB}$, where $|H\rangle$ and $|V\rangle$ denote the horizontal and vertical polarization states, respectively. Then the state after passing through the two quartz plates is

$$\begin{aligned}|\psi^f\rangle = {}& \frac{1}{\sqrt{2}}|HV\rangle_{AB} \\ & \otimes \int g(\omega_1,\omega_2)e^{i(\omega_1 n_H L_1+\omega_2 n_V L_2)/c}|\omega_1\rangle_A|\omega_2\rangle_B d\omega_1 d\omega_2 \\ & + \frac{1}{\sqrt{2}}|VH\rangle_{AB} \\ & \otimes \int g(\omega_1,\omega_2)e^{i(\omega_1 n_V L_1+\omega_2 n_H L_2)/c}|\omega_1\rangle_A|\omega_2\rangle_B d\omega_1 d\omega_2.\end{aligned}$$

And the density matrix of the two-photon polarization state can be figured out by tracing the frequency DOF:

$$\begin{aligned}\rho^f_{\text{pol}} &= \text{Tr}_{\omega_1\omega_2}(|\psi^f\rangle\langle\psi^f|) \\ &= \frac{1}{2}|HV\rangle\langle HV| + \frac{1}{2}|VH\rangle\langle VH| \\ &\quad + \frac{1}{2}|HV\rangle\langle VH| \int |g(\omega_1,\omega_2)|^2 \\ &\quad \times e^{i(\omega_2 L_2-\omega_1 L_1)\triangle n/c} d\omega_1 d\omega_2 \\ &\quad + \frac{1}{2}|VH\rangle\langle HV| \int |g(\omega_1,\omega_2)|^2 \\ &\quad \times e^{i(\omega_1 L_1-\omega_2 L_2)\triangle n/c} d\omega_1 d\omega_2.\end{aligned}$$

Here we make an assumption that the frequency filters for photons A and B have narrow bandwidth, such that

$$n_V(\omega_1) - n_H(\omega_1) \approx n_V(\omega_2) - n_H(\omega_2) = \triangle n$$

for all ω_1 and ω_2 in the bandwidth. Recalling the requirement in Ref. [20] for the decoherence model to be exchange-symmetric, we should further require that $L_1 = L_2 = L$, $h_A(\omega) = h_B(\omega) = h(\omega)$, and $a_p(\omega_p)$ is a white spectrum. Thus the decoherence "environments" that photons A and B endure are identical and independent, i.e., exchange-symmetric. So the final density matrix of the 2-qubit state in the polarization DOF is given as (based on $|HH\rangle$, $|HV\rangle$, $|VH\rangle$, $|VV\rangle$)

$$\rho^f_{|\Psi\rangle^+_{AB}}(L) = \begin{pmatrix} 0 & 0 & 0 & 0 \\ 0 & \frac{1}{2} & \frac{1}{2}G(L) & 0 \\ 0 & \frac{1}{2}G^*(L) & \frac{1}{2} & 0 \\ 0 & 0 & 0 & 0 \end{pmatrix},$$

where

$$G(L) = \int |h(\omega_1)h(\omega_2)a_p(\omega_p)|^2 e^{i(\omega_2-\omega_1)\triangle n L/c} d\omega_1 d\omega_2.$$

Similar calculations for the other three Bell states yield

$$\rho^f_{|\Phi\rangle^+_{AB}}(L) = \begin{pmatrix} \frac{1}{2} & 0 & 0 & \frac{1}{2}G_1(L) \\ 0 & 0 & 0 & 0 \\ 0 & 0 & 0 & 0 \\ \frac{1}{2}G_1^*(L) & 0 & 0 & \frac{1}{2} \end{pmatrix},$$

$$\rho^f_{|\Phi\rangle^-_{AB}}(L) = \begin{pmatrix} \frac{1}{2} & 0 & 0 & -\frac{1}{2}G_1(L) \\ 0 & 0 & 0 & 0 \\ 0 & 0 & 0 & 0 \\ -\frac{1}{2}G_1^*(L) & 0 & 0 & \frac{1}{2} \end{pmatrix},$$

$$\rho^f_{|\Psi\rangle^-_{AB}}(L) = \begin{pmatrix} 0 & 0 & 0 & 0 \\ 0 & \frac{1}{2} & -\frac{1}{2}G(L) & 0 \\ 0 & -\frac{1}{2}G^*(L) & \frac{1}{2} & 0 \\ 0 & 0 & 0 & 0 \end{pmatrix},$$

where

$$G_1(L) = \int |h(\omega_1)h(\omega_2)a_p(\omega_p)|^2 e^{-i(\omega_2+\omega_1)\triangle nL/c} d\omega_1 d\omega_2.$$

In the following we will discuss the exchange-symmetry property of the state after decoherence. Notice that there is only one exchange-antisymmetric state in the four Bell states, and the other three Bell states are all exchange-symmetric. We can conclude that among all 2-qubit pure states, there is only one exchange-antisymmetric state, i.e., $|\Psi^-\rangle$. So we use the following definition as a measure for the exchange-symmetry property:

$$S = 1 - \langle\Psi^-|\rho^f(L)|\Psi^-\rangle.$$

Figure 1 shows the theoretical results of S versus scaled quartz thickness N ($N = \triangle nL/\lambda_0$; $\lambda_0 = 780$ nm; L is quartz length) for $|\Phi\rangle^\pm_{AB}$ and $|\Psi\rangle^\pm_{AB}$ with different $h(\omega)$ and $a_p(\omega_p)$. For $|\Phi\rangle^\pm_{AB}$, the values of S remain unchanged when L changes. and it is also obvious that S will not change with different $h(\omega)$ and $a_p(\omega_p)$ for $|\Phi\rangle^\pm_{AB}$, because their expressions of S do not contain any factor of $G_1(L)$. However, the situations for $|\Psi\rangle^\pm_{AB}$ are more complex. We can see from Figs. 1(c)–1(h) that for $|\Psi\rangle^+_{AB}(|\Psi\rangle^-_{AB})$, the values of S always decrease (increase) from 1 (0) to 0.5 at an asymptotic limit. But the details of these processes are not the same when $h(\omega)$ and $a_p(\omega_p)$ change. When $h(\omega)$ has a Gaussian shape, the curves of S are identical no matter whether $a_p(\omega_p)$ is a white spectrum or a delta function $\delta(\omega_p - \omega_{p0})$ [see Figs. 1(c) and 1(d)]. If $h(\omega)$ has a rectangular shape, the values of S break through the limit of 0.5 in some regions of L when $a_p(\omega_p)$ is $\delta(\omega_p - \omega_{p0})$ [see Figs. 1(e) and 1(f)] And if we apply the real transmission spectrum of the interference filter used in our experiment for $h(\omega)$, we get results like those in Figs. 1(c) and 1(d) [see Figs. 1(g) and 1(h)], because the interference filter we used has an approximately rectangular transmission spectrum. In a real experiment, we cannot provide a pump light with white spectrum as required for the exchange-symmetric decoherence model. So we can deduce from our experiment results whether it is a good approximation to take our experiment decoherence model as an exchange-symmetric one by checking whether the measured values of S exceed the limit 0.5 when L increases.

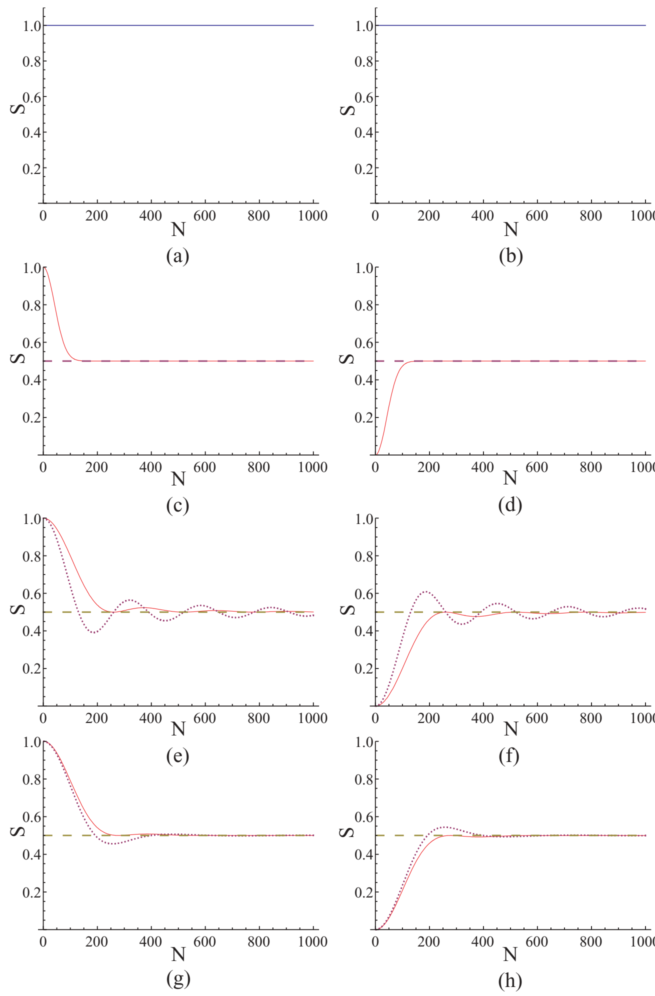

FIG. 1. (Color online) Theoretical calculated results of S versus quartz plate length N for four Bell states with different $h(\omega)$ and $a_p(\omega_p)$. Panels (a) and (b) are for $|\Phi\rangle^+$ and $|\Phi\rangle^-$, respectively, and the curves are both $S = 0.5$ for all kinds of $h(\omega)$ and $a_p(\omega_p)$. Panels (c), (e), and (g) are for $|\Psi\rangle^+$, with $h(\omega)$ being a Gaussian spectrum, rectangular spectrum, and our experiment's filter spectrum, respectively; while (d), (f), and (h) are for $|\Psi\rangle^-$, with $h(\omega)$ being the same as (c), (e), and (g), respectively. The dashed lines at $S = 0.5$ in (c)–(h) show the asymptotic limit. In (c) and (d), the S curves when $a_p(\omega_p)$ being white spectrum and delta function $\delta(\omega_p - \omega_{p0})$ are identical, so we see only one curve in each figure. In (e)–(h), the dotted lines show the $a_p(\omega_p)$ curves for for the delta function, while the solid lines show the $a_p(\omega_p)$ curves for the white spectrum.

III. EXPERIMENT SETUP AND RESULTS

Our experiment setup is shown in Fig. 2. A pulse train from a mode-locked Ti : sapphire laser (with a duration of 140 fs, a repetition rate of 76 MHz, and a central wavelength of 780 nm) is frequency-doubled, and the output ultraviolet laser beam of the frequency doubler is focused onto one pair of β barium borate (BBO) crystals for down-conversion. The two BBO crystals are both 1 mm thick and cut at $\theta_{\rm pm} = 42.62^\circ$, $\varphi = 30^\circ$ for beamlike two-photon generation [25,26], and they are oriented in a special way to prepare the two-photon Bell state in the polarization DOF, while some specially designed birefringent crystals are placed in the paths of down-converted photons for time and spatial compensation [27]. Then, two polarization-preserved single-mode fibers transfer the prepared two-photon initial states to the decoherence part of the experiment. Using the half-wave plate (HWP) and tiltable quarter-wave plate (QWP), we can easily transform one Bell state to another. The entanglement interference visibility of our prepared Bell state is $V = (96.8 \pm 0.8)\%$. And two-photon coincidence rates based on $|HV\rangle$ and $|VH\rangle$ are about 16 000 pairs/s for 50-mW pump laser power.

In the decoherence part, we set the paths of the two photons parallel and very close to each other so that they can pass through the same piece of quartz plate. This small trick can ensure that the two local paths imposed by the quartz on the two photons are identical. This trick is also critical for the measurements in cases of $|\Psi\rangle^\pm_{AB}$, because very small differences in quartz length (of the order of $L = \lambda_0/\triangle n$) will introduce a relative phase between the $|HV\rangle$ and $|VH\rangle$ terms of $|\Psi\rangle^\pm_{AB}$, thus leading to additional variations of S.

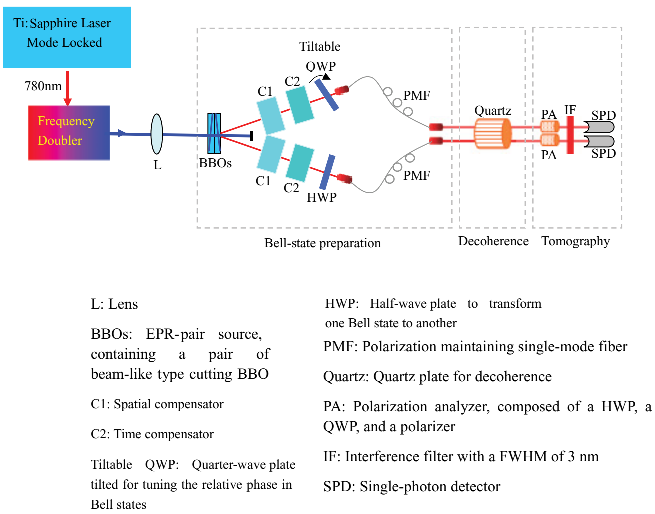

FIG. 2. (Color online) Experiment setup for Bell states preparation, decoherence, and final-state tomography.

For example, when $L_A = 0$ and $L_B = \frac{\lambda_0}{2(n_V - n_H)}$, almost no decoherence happens, but the value of S will directly change from 1 to 0 (or from 0 to 1) for $|\Psi\rangle_{AB}^{+}(|\Psi\rangle_{AB}^{-})$. Such variations might lead to confusion about the phenomena we want to observe in this experiment. In the decoherence part, the optic axis of the quartz plate is set to be parallel to the vertical polarization direction of the down-converted photon. So for our central wavelength $\lambda_0 = 780$ nm, $n_V = n_e = 1.54769$, and $n_H = n_o = 1.53879$. Finally, the output two-photon state from the decoherence part is directed into a two-photon polarization-state tomography device, which consists of two sets of polarization analyzers.

Figure 3 illustrates the experimentally measured S values of different lengths of quartz plates for the four cases. The scaled quartz lengths N we employed in the experiment are $N = 0, 34, 58, 75, 92, 109, 133, 150, 167, 184, 199, 216, 233,$ and 274, respectively. We can see that the results agree well with the theoretically calculated curves. The typical error of S in Fig. 3 is about ± 0.025. As mentioned in Sec. II, in a real experiment we cannot provide a pump light with a white spectrum, so we use an ultrashort pulse laser (pulse width less than 200 fs) as the pump for SPDC instead, which has a Gaussian spectrum and a relatively larger bandwidth. In such a condition we consider the two local decoherence paths to be approximately independent, thus leading to an exchange-symmetric decoherence model.

By checking the measured results for $|\Psi\rangle_{AB}^{\pm}$, we can see that no value of S breaks through the limit of 0.5, indicating that our result is closer to the S curve when $a_p(\omega_p)$ being white-spectrum in Figs. 1(g) and 1(h); thus the decoherence model in our experiment can be considered an exchange-symmetric one. So the results

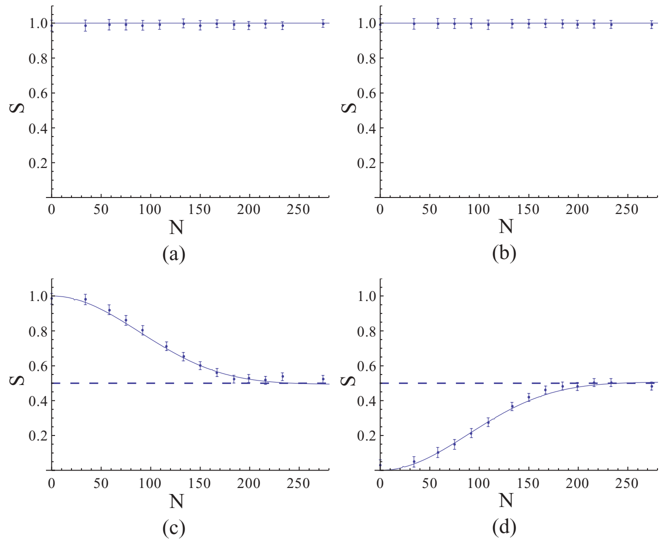

FIG. 3. (Color online) Experimentally measured S values versus scaled quartz length N for four Bell states: (a) $|\Phi\rangle^{+}$, (b) $|\Phi\rangle^{-}$, (c) $|\Psi\rangle^{+}$, (d) $|\Psi\rangle^{-}$. Solid curves are theoretically calculated S values with our experiment's filter transmission spectrum and pump light's practical spectrum. The dashed lines in (c) and (d) are the asymptotic limit of $S = 0.5$.

for $|\Psi\rangle_{AB}^{+}$ provide some evidence to support the effect of decoherence-induced spontaneous symmetry breaking.

IV. CONCLUSION

In summary, we experimentally investigated the evolution of the exchange-symmetry property for Bell states under an exchange-symmetric decoherence model. Our experiment results show some evidence supporting the effect of decoherence-induced spontaneous symmetry breaking. However, to conclusively show this effect, more work is needed. To our knowledge, no experiments have investigated the relation between decoherence and symmetry reported before. Our results might be helpful for a deeper understanding of decoherence in the future.

ACKNOWLEDGMENTS

This work was supported by the National Fundamental Research Program (2006CB921907), National Natural Science Foundation of China (Grants No. 11074242 and No. 10874162), Innovation Funds from Chinese Academy of Sciences (CAS), Program for New Century Excellent Talents in University, International Cooperation Program from CAS and Ministry of Science and Technology of China, and the Foundation for the Author of National Excellent Doctoral Dissertation of People's Republic of China (Grant No. 200729).

[1] E. Schrödinger, Proc. Cambridge Philos. Soc. **31**, 555 (1935).
[2] C. H. Bennett, G. Brassard, C. Crépeau, R. Jozsa, A. Peres, and W. K. Wootters, Phys. Rev. Lett. **70**, 1895 (1993).
[3] A. K. Ekert, Phys. Rev. Lett. **67**, 661 (1991).
[4] A. Muller, H. Zbinden, and N. Gisin, Europhys. Lett. **33**, 335 (1996).
[5] C. H. Bennett and S. J. Wiesner, Phys. Rev. Lett. **69**, 2881 (1992).

[6] D. Deutsch and R. Josza, Proc. R. Soc. London A **439**, 553 (1992).
[7] P. W. Shor, SIAM J. Comput. **26**, 1484 (1997).
[8] M. A. Nielson and I. L. Chuang, *Quantum Computation and Quantum Information* (Cambridge University Press, Cambridge, England, 2000).
[9] L.-M. Duan, M. D. Lukin, J. I. Cirac, and P. Zoller, Nature (London) **414**, 413 (2001).
[10] E. Knill, R. Laflamme, and G. J. Milburn, Nature (London) **409**, 46 (2001).
[11] W. H. Zurek, Rev. Mod. Phys. **75**, 715 (2003).
[12] T. Yu and J. H. Eberly, Phys. Rev. B **66**, 193306 (2002).
[13] D. Tolkunov, V. Privman, and P. K. Aravind, Phys. Rev. A **71**, 060308(R) (2005).
[14] Z. Gedik, Solid State Commun. **138**, 82 (2006).
[15] A. G. Kofman and A. N. Korotkov, Phys. Rev. A **77**, 052329 (2008).
[16] M. Horodecki, P. Horodecki, and R. Horodecki, in *Quantum Information: An Introduction to Basic Theoretical Concepts and Experiments*, edited by G. Alber, Springer Tracts in Modern Physics, Vol. 173 (Springer-Verlag, Berlin, 2001).
[17] J. van Wezel, J. van den Brink, and J. Zaanen, Phys. Rev. Lett. **94**, 230401 (2005).
[18] T. Birol, T. Dereli, and Ö. E. Müstecaplıoğlu, and L. You, Phys. Rev. A **76**, 043616 (2007).
[19] J. van Wezel, J. Zaanen, and J. van den Brink, Phys. Rev. B **74**, 094430 (2006).
[20] G. Karpat and Z. Gedik, Opt. Commun. **282**, 4460 (2009).
[21] P. G. Kwiat, A. J. Berglund, J. B. Altepeter, and A. G. White, Science **290**, 498 (2000).
[22] A. J. Berglund, "Quantum coherence and control in one- and two-photon optical systems." 2000, e-print arXiv:quant-ph/0010001v2.
[23] F. W. Sun, B. H. Liu, Y. F. Huang, Y. S. Zhang, Z. Y. Ou, and G. C. Guo, Phys. Rev. A **76**, 063805 (2007).
[24] Y.-S. Zhang, Y.-F. Huang, C.-F. Li, and G.-C. Guo, Phys. Rev. A **66**, 062315 (2002).
[25] S. Takeuchi, Opt. Lett. **26**, 843 (2001).
[26] C. Kurtsiefer, M. Oberparleiter, and H. Weinfurter, J. Mod. Opt. **48**, 1997 (2001).
[27] X.-L. Niu, Y.-F. Huang, G.-Y. Xiang, G.-C. Guo, and Z. Y. Ou, Opt. Lett. **33**, 968 (2008).